Synthetic Metals 234 (2017) 132–138

Contents lists available at ScienceDirect

Synthetic Metals

journal homepage: www.elsevier.com/locate/synmet

Research paper

Design and chiroptical properties of a water-soluble and violet-blue emissive alkyne template

Tingchao He[a,b,1], Yi Zhang[a,1], Song Yao[a], Xingrong Li[a], Fenghuan Zhao[c], Xiaodong Lin[a], Jiuxu Xia[d], Wei Lu[d], Chuanxiang Ye[a], Rui Chen[c,*], Junmin Zhang[a,*]

[a] College of Physics and Energy & College of Chemistry and Environmental Engineering, Shenzhen University, Shenzhen 518060, China
[b] Key Laboratory of Optoelectronic Devices and Systems of Ministry of Education and Guangdong Province, Shenzhen University, Shenzhen 518060, China
[c] Department of Electrical and Electronic Engineering, South University of Science and Technology of China, Shenzhen 518055, China
[d] Department of Chemistry, South University of Science and Technology of China, Shenzhen 518055, China

ARTICLE INFO

Keywords:
Alkyne architecture
Circular dichroism
Circular polarized luminescence
Two-photon circular dichroism

ABSTRACT

Circular dichroism (CD) and circular polarized luminescence (CPL) are useful for various applications. However, it is difficult to achieve excellent CD and CPL in differently polar solvents simultaneously. This work provides a simple but efficient way to construct violet-blue fluorescent and water-soluble chromophore through the construction of rigid conformation of the alkyne architecture. By introducing proline pendants into alkyne architecture, the chromophore exhibits reasonable CD and CPL properties in the lowly and highly polar solvents. More importantly, even in water, the chromophore displays effective CD anisotropy factor ($g_{abs} \sim 1 \times 10^{-3}$) and luminescence dissymmetry factor ($g_{lum} \sim 2 \times 10^{-3}$), as well as high fluorescence quantum yield (Φ up to 35%). Additionally, the chromophore exhibits large two-photon CD according to the theoretically calculated results. The excellent chiroptical properties from the simple organic fluorophore enables its future applications in miniatured optoelectronic devices and CPL-based bioimaging.

1. Introduction

Recently, chiroptical phenomena, including circular dichroism (CD) and circularly polarized luminescence (CPL), have received growing interest due to the development of smart photonic materials for advanced technologies [1–9]. CD measurements are used to reveal the chirality of ground state molecules, while applications of CPL have primarily been used to obtain structural information about molecular excited states [10]. More importantly, there has been a growing interest in developing optical materials that are capable of emitting CPL because of their potential applications in information storage and processing, 3D displays, spintronics-based devices, biological probes and signatures, security tags, CPL lasers, enantioselective CPL sensors and CPL microscopes [1,2,11–14].

So far, there have been lots of reports on various CD and CPL materials, such as lanthanide complexes [15], conjugated polymers [16], metal nanoparticles [17], semiconductor quantum dots [18], simple organic molecules [19], and so on. Although there are numerous examples of optical materials that show reasonable chirality in organic solvents or solid state, previous literatures reported their chiral behaviors in only one or two media [20,21]. The influences of solvent polarity on CD and CPL of materials have been rarely explored. Even though there are occasional chiral materials investigated in different two solvents, they suffer from serious attenuation of chiroptical behaviors in highly polar media, especially in water [22]. It is not beneficial for extending their chiroptical applications.

From the viewpoint of applications, chiral optoelectronic devices are likely to be exposed to complicated environments, so the robust chirality of materials again environmental alteration, such as solvent polarity, should be extremely important. Therefore, there is an urgent requirement to develop simple molecules with reasonable or robust chirality in differently polar solvents. To the best of our knowledge, there are few chiral materials exhibiting reasonable CD and CPL dissymmetry factors ($> 1 \times 10^{-3}$) in different media ranging from lowly to highly polar solvents. Except aggregation induced chiral molecular self-assembled structures [23,24], scarce organic simple molecules shows effective luminescence quantum yield (QY, $\Phi > 30\%$) in water. The development of such kinds of simple molecules is of great importance, since they would be active chiral materials for various potential applications. Therefore, research guidelines directed toward the

* Corresponding authors.
E-mail addresses: chen.r@sustc.edu.cn (R. Chen), zhangjm@szu.edu.cn (J. Zhang).
[1] Equal contributions.

http://dx.doi.org/10.1016/j.synthmet.2017.10.008
Received 7 April 2017; Received in revised form 21 September 2017; Accepted 16 October 2017
Available online 05 November 2017
0379-6779/

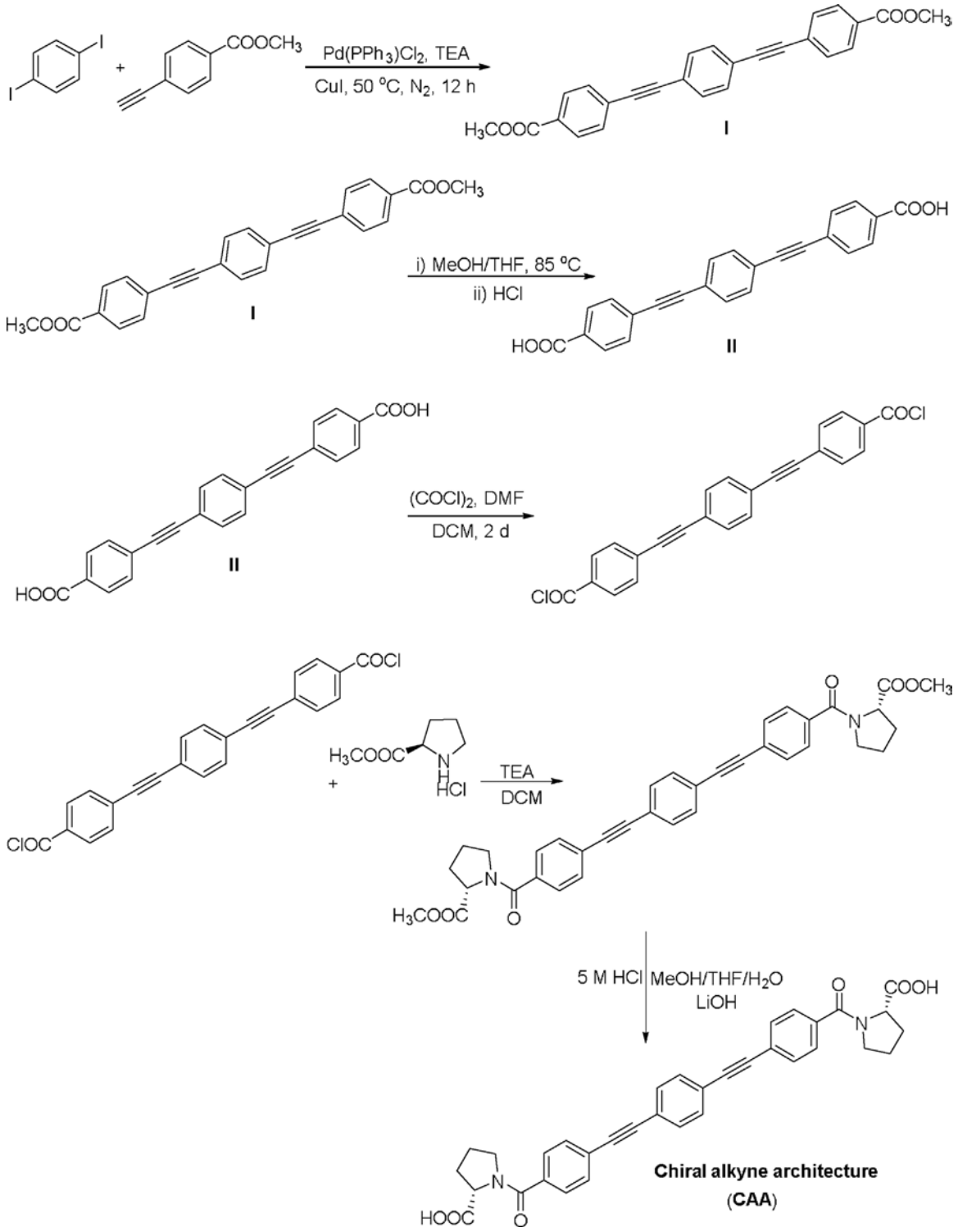

Scheme 1. The synthesis protocol of the chiral alkyne architecture (4,4′-(1,4-phenylenebis(ethyne-2,1-diyl))bis(benzoyl))diproline).

expansion of organic molecules enabling excellent CD and CPL in various organic solvents are urgently needed.

In this work, we report the design and synthesis of one novel chiral alkyne architecture, which is covalently tethered by two identical chiral proline pendants. Interestingly, the chromophore shows efficient CD and CPL behaviors in differently polar solvents. Especially, no obvious attenuation of CPL properties has been observed in water, which we believe should have a broad range of potential applications. Additionally, the theoretically calculated results indicate the chromophore exhibits large two-photon CD (TP-CD), which is defined as the difference between two-photon absorption (TPA) for left and right circular polarization light, respectively. Therefore, the chromophore is a useful TP-CD probe and has unique fingerprinting functionality for chiral species.

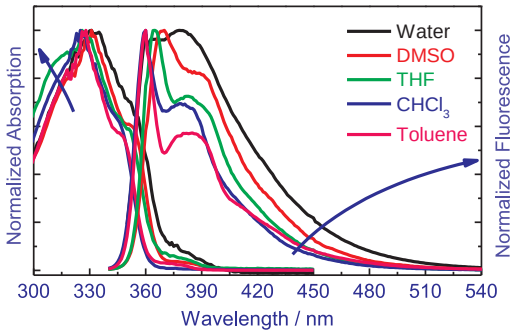

Fig. 1. Normalized absorption and fluorescence emission spectra of the chiral alkyne architecture in different organic solvents.

2. Methods and characterization techniques

2.1. Material synthesis

The synthesis protocol of the chiral alkyne architecture is depicted in Scheme 1. The detailed processes and characterizations are described as follows. Methyl 4-ethynylbenzoate (2.0 g) was dissolved in triethylamine (300 mL) by stirring. The obtained solution was degassed for 10 min. After that, 1,4-diiodobenzene (2.0 g), bis(triphenylphosphine) palladium(II) dichloride (0.3 g) and copper(I) iodide (0.1 g) were added. The reaction mixture was stirred at 50 °C for 12 h under N_2 atmosphere. After cooling to room temperature, the product was collected by filtration and was washed with hexane for two times to afford white solid compound **I** (2.1 g). The compound **I** was dissolved in MeOH/THF (V/V = 1:1). The resultant solution was allowed to reflux overnight at 85 °C. After cooling to room temperature, the product was precipitated by addition of 5 M HCl. The slightly colored solid compound **II** (1.7 g) was obtained by filtration and washing with water.

The compound II (0.9 g) was then dissolved in dry DCM (100 mL) and one drop of DMF was added. The resultant solution was degassed with N_2 for three times. Subsequently, oxalyl chloride (4 equiv.) was added slowly and the obtained solution was stirred for 2 days at 25 °C. After the solvent was evaporated, dry DCM (100 mL) and triethylamine (10 equiv.) were added. Then methyl L-prolinate hydrochloride (2.1 equiv.) was added after the reaction solution was degassed with N_2. The reaction mixture was stirred overnight under room temperature. After evaporating solvent, white solid was obtained, which was washed with water for three times and was dissolved in MeOH/THF/H_2O ($V/V/V$ = 1:1:1). LiOH (1.05 equiv.) was then added to the obtained solution and was stirred for 1 h at 0 °C. After that, 5 M HCl was dropped into reaction mixture until the pH = 7. White solid was received through filtration and was washed with water for three times. Finally, the obtained solid was purified by recrystallization to afford white power 0.6 g (43%) as the target product chiral alkyne architecture ((4,4′-(1,4-phenylenebis(ethyne-2,1-diyl))bis(benzoyl))- diproline, abbreviated as **CAA**). NMR and HRMS spectra were then recorded (Figs. S1–S3).

^{1}H NMR (400 MHz, DMSO-d_6): δ 12.60 (s, 2H), 7.66 (d, J = 8.3 Hz, 6H), 7.59 (d, J = 8.1 Hz, 4H), 7.44 (d, J = 8.0 Hz, 1H), 4.40 (dt, J = 16.5, 8.1 Hz, 1H), 3.65–3.55 (m, 1H), 3.55–3.44 (m, 2H), 2.28 (d, J = 8.7 Hz, 1H), 2.03–1.75 (m, 4H).

^{13}C NMR (100 MHz, DMSO-d_6): δ 173.16, 167.36, 136.43, 131.81, 131.29, 127.07, 123.57, 122.39, 90.83, 90.21, 59.00, 49.43, 28.93, 25.00.

HRMS-ESI (m/z) calcd for $C_{34}H_{28}N_2O_6$ ($[M + H]^+$): 561.2026, found 561.2028.

2.2. Photophysical methods

The measurements of linear absorption, fluorescence and QYs. The solutions were filled into quartz cuvettes with 1 cm path length. UV–vis absorption and fluorescence spectra of the samples were measured by using a Lambda 950 UV/Vis spectrometer (PerkinElmer, Inc.) and a Zolix fluorescence spectrophotometer (SENS-9000), respectively. The absolute QYs of targeted compound in different solvents were determined by using an integrating sphere equipped Zolix fluorescence spectrophotometer.

Lifetime measurements. The values of lifetime were determined at room temperature using Hamamatsu compact luminescence lifeline spectrometer C11367 with a C11367-11 photomultiplier tube. A LED light source (365 nm, 1 MHz repetition rate) was used as the excitation source.

CD and CPL measurements. CD and CPL spectra were recorded at room temperature using JASCO J-1500 and CPL-300 spectrometers, respectively. Quartz cuvettes with a 1 cm path length, which are filled with solutions with concentration of 1×10^{-5} M, are used for all CD and CPL experiments. Each CD or CPL spectrum was measured with an average of at least 15 scans.

2.3. Theoretical calculations

The molecular structure was optimized using density functional theory (DFT), employing B3LYP hybrid functional and the 6–31G* basis set in Gaussian 09. The TP-CD spectrum of the optimized molecular structure was obtained with the same correlation exchange functional and basis set in DALTON 2011.

3. Results and discussion

3.1. Steady-State spectroscopic measurements of the chiral alkyne architecture

To examine the electronic structure of chiral alkyne architecture, absorption spectra of the chromophore were measured in differently polar solvents, such as toluene, $CHCl_3$, THF, acetone, DMSO and water. It is noteworthy that the water solubility of chiral alkyne architecture can be up to 1×10^{-4} M. The normalized absorption and emission spectra of the chromophore in different solvents are shown in Fig. 1. It could be known that the shapes of the absorption spectra of the compound were very similar and displayed intense absorption bands located around at 328 and 350 nm. Compared with the experimental results, the spectral lineshape of absorption spectrum can be well produced by the theoretical computation except for a red shift of 57 nm (Fig. S4). It was found that both the absorption and emission spectra were a little sensitive to the changes in the polarity of the environment, with wavelength shift of several nanometers. It is worth noting that the chromophore exhibits dual absorption and emission wavelengths in different solvents, which should originate from vibrionic bands (0−0', 0−1'). Additionally, the emission spectra display more pronounced dual emission bands and the QYs of the chromophore decrease as the solvent polarity increases. However, it still remains a high value in water, as high as 35%. The photophysical parameters for the chromophore in different solvents, such as absorption and emission wavelengths, as well as QYs, are listed in Table 1. The high QYs of the chromophore in different solvents are mainly caused by strong structural rigidity, which is further confirmed by molecular small Stokes shifts. Actually, the influences of solvent polarity on the photophysical properties of chromophores, such as emission wavelength and QY, have been widely studied. There are various chromophores exhibiting efficient intramolecular charge transfer (ICT) and displaying broad tunability of fluorescence wavelength and QY. The related values of many chromophores can change by more than 100 nm and one order of magnitude, respectively [25–30]. However, in our case, the tunability is much smaller, that is, several nanometers and 30%. Therefore, compared to previous chromophores, the ICT properties of our chromophore are much weaker.

We have calculated various frontier orbitals of the chromphore

Table 1
Experimental photophysical properties of the chiral alkyne architecture in different solvents.

Solvent[a]	λ_{abs}[b] (nm)	λ_{ems}[c] (nm)	τ[d] (ns)	Φ[e] (%)	g_{abs}[f]	g_{lum}[g]
Toluene	325, 345	360, 384	1.63	79	1.5×10^{-3}	3.6×10^{-3}
$CHCl_3$	326, 345	361, 384	1.49	72	1.6×10^{-3}	1.9×10^{-3}
THF	328, 350	365, 386	1.24	30	0.6×10^{-3}	0.4×10^{-3}
DMSO	331, 353	370, 390	1.25	33	0.1×10^{-3}	0.7×10^{-3}
H_2O	333, 355	365, 380	1.23	35	1.0×10^{-3}, -0.8×10^{-3}	2.0×10^{-3}

[a] Concentration was estimated as 1×10^{-5} M in related measurements.
[b] Absorption maximum.
[c] Fluorescence emission maximum; The dual absorption and emission wavelengths of the chromophore in different solvents originate from vibrionic bands (0-0′, 0–1′).
[d] Fuorescence lifetime under the excitation of 365 nm.
[e] Absolute QY values measured by using an integrating sphere.
[f] Dissymmetry ratio of CD.
[g] Dissymmetry ratio of CPL.

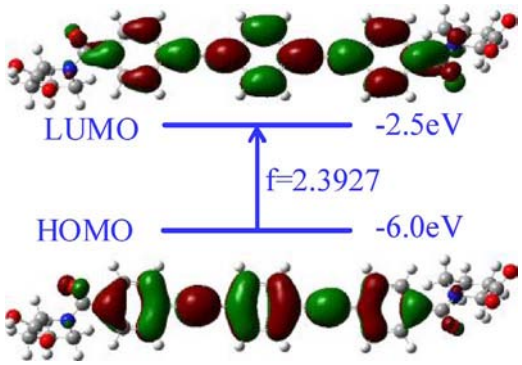

Fig. 2. Optimized frontier HOMO/LUMO of chiral alkyne architecture calculated with DFT at the B3LYP/6-31G(d) level by applying the Gaussian 09 program. The color dots represent electron cloud.

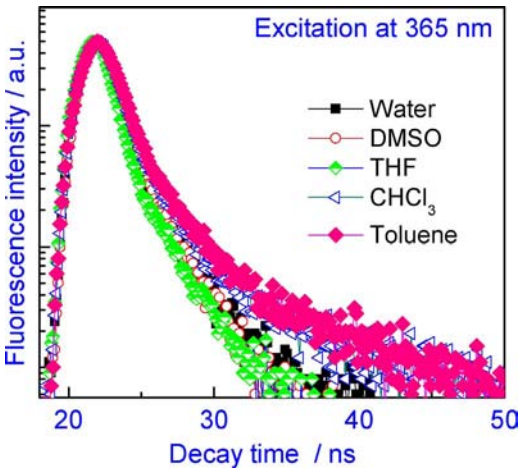

Fig. 3. Fluorescence decay profiles of chiral alkyne architecture (λ_{ex} = 365 nm).

(Figs. S5 and S6). From the corresponding calculated parameters, it can be known that the molecular orbitals of the highest occupied molecular orbital (HOMO) and lowest unoccupied molecular orbital (LUMO) mainly contribute to the observed absorption spectra, which will then contribute to the CD or CPL behaviors that will be discussed later. Therefore, only HOMO and LUMO are displayed, where color dots represent electron cloud (Fig. 2). Additionally, we have added the corresponding oscillator strength (f) and energy values of HOMO and LUMO. Obviously, there is a negligible change in the electron density of HOMO and LUMO, indicating weak ICT behavior. It is consistent with

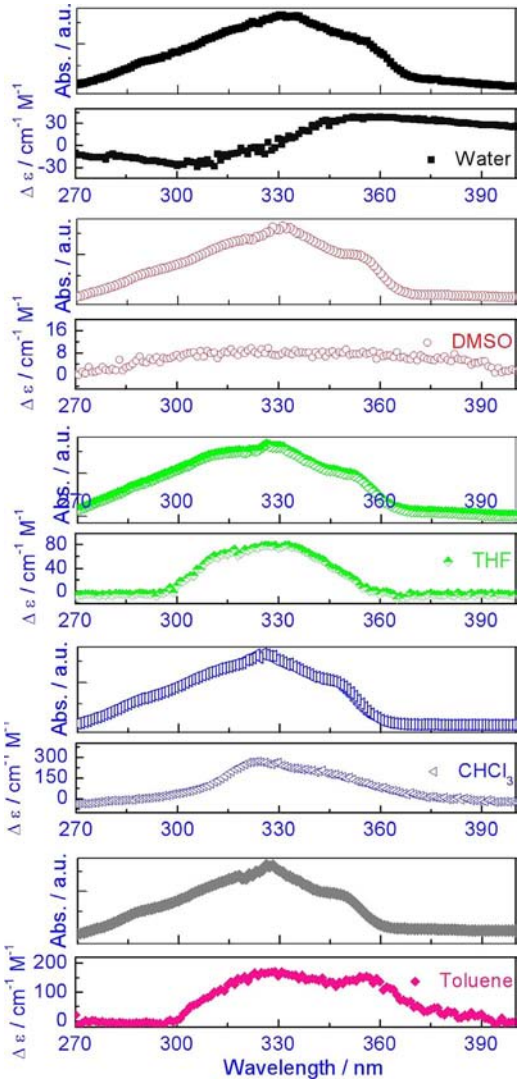

Fig. 4. Comparison of CD and absorption spectra for the chromophore in different solvents.

the experimental results. Although the accurate reasons why dual emission bands vary in different solvents remain unclear, they may be due to the formation of locally excited state and twisted ICT state [31,32].

3.2. Measurements of fluorescence lifetimes of the chiral alkyne architecture

To evaluate the excited state dynamics of the compound in different solvents, fluorescence lifetime measurements were performed. The fluorescence decay profiles are shown in Fig. 3. The compound exhibits double-exponential fluorescence decay behavior in all the solvents, thus indicating strong intermolecular interaction between chromophore and solvent [33,34]. The shorter lifetime (τ) component of decay process can be attributed to a nonradiative decay pathway. The values of average fluorescence lifetime were evaluated from exponential fits and are summarized in Table 1. For the chromophores with efficient ICT, the lifetime will strongly depend on the solvent polarities. The values of lifetime can vary by more than one order of magnitude [35–37]. The lifetime of chiral alkyne architecture in highly polar solvent (1.23 ns in water) is only slightly shorter than that in case of lowly polar solvent (1.63 ns in toluene). Again, the obtained results indicated that the calculated lifetime values correlated with the polarity insensitive emission behaviors.

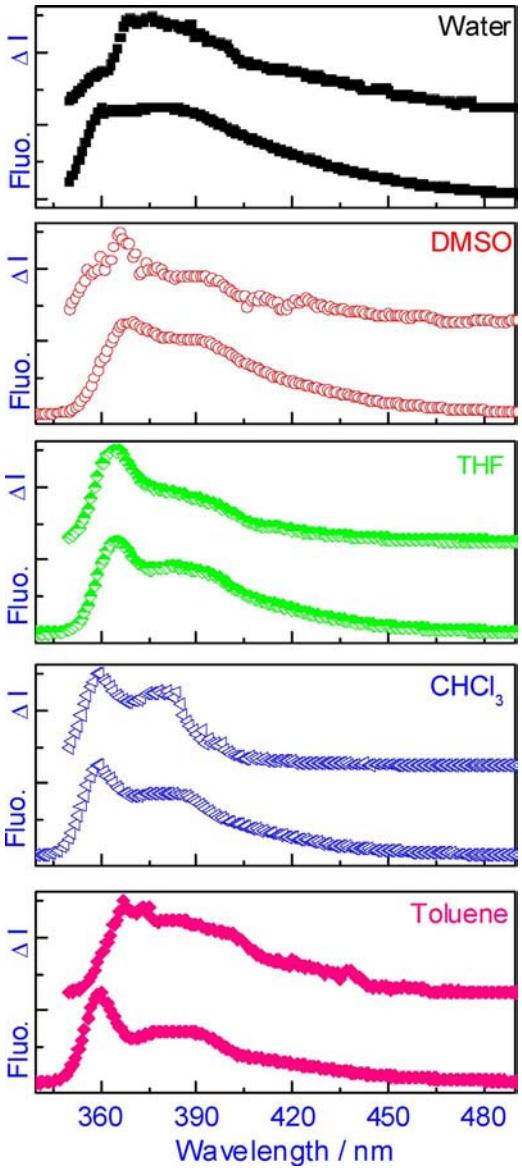

Fig. 5. Comparison of CPL (ΔI) and fluorescence (Fluo.) spectra for the chromophore in different solvents, upon excitation at 330 nm.

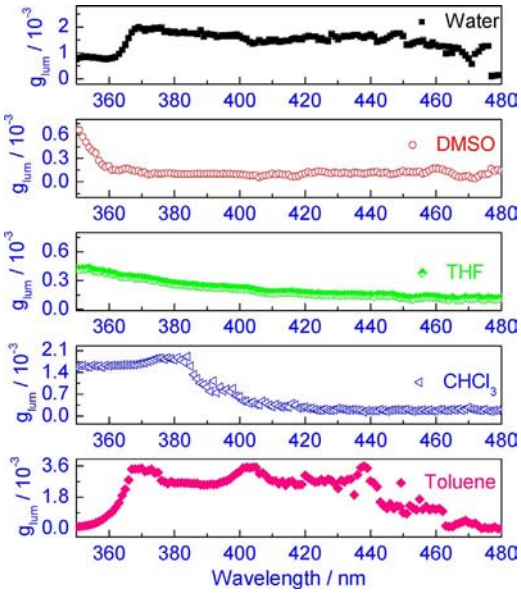

Fig. 6. Luminescence dissymmetric factor (g_{lum}) for the chromophore in different solvents as a function of emission wavelength.

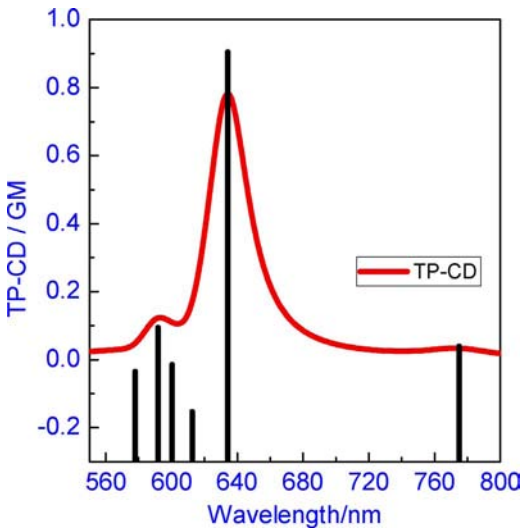

Fig. 7. TP-CD spectrum of the chromophore obtained from theoretical calculations. The simulated CD spectrum is generated as sums of Lorentz with σ = 0.1 eV, in which vertical bars represent rotational strengths (in arbitrary absolute unit).

3.3. CD spectra of chiral alkyne architecture

Fig. 4 depicts the comparison of CD and absorption spectra for the chromophore in different solvents. It can be seen that the CD spectrum of the chromophore in water is different from other spectra. To be specific, the water solution displays a bisignate trace while the spectra for other solvents don't exhibit such a behavior. It is also found that in toluene, $CHCl_3$, THF and DMSO strong Cotton effect was observed for the chromophore between 300 and 400 nm, demonstrating that the designed chiral perturbation of proline is indeed acting on the alkyne architecture, at least in its ground state. There are distinct differences between experimental and theoretically calculated spectra, such as spectral lineshape and peak wavelength (Fig. S7), which are due to the reasons that the environmental factors including solvent effect, temperature and so on, have not been taken into consideration and the calculations of absorption and CD only employ the vertical excitation approximation. To evaluate the chiroptical dissymmetry of the alkyne architecture, we calculated its CD anisotropy factors (g_{abs}). The CD anisotropy factor is defined as $g = \Delta\varepsilon/\varepsilon = (A_L - A_R)/A$, where A represents the conventional absorbance of nonpolarized light and A_L and A_R are the absorption of left and right circularly polarized light, respectively [38]. The CD anisotropy factor is independent of the concentration and path length, since the absorbance of sample is taken into consideration. The maximum values of g_{abs} in different solvents were determined in range from 0.1×10^{-3} to 1.6×10^{-3}. These g_{abs} values are larger than those of many simple molecules [11,39,40], even comparable to lots of chiral aggregates [41,42].

It is known that chiroptical properties are sensitive to molecular environment, owing to the presence of different interactions between the chromophore and solvent. Additionally, the solubility of chromophore in different solvents can also influence the molecular chiroptical properties. In some solvents the chromophore can exist as individual one, while it suffers from slight aggregation in other solvents. As a result, the molecular conformation will depend on the polarity of the solvent and the chromophore has a tendency to undergo polarity dependent chiroptical properties [43,44]. In our case, the alkyne architecture exhibits larger chiroptical properties in lowly polar solvents compared to the highly polar ones. However, in aqueous solution, the

chiroptical behavior increases again, probably by virtue of strong interactions between the chromophore and water molecule and subsequent formation of aggregates and exciton coupling effect [45]. It is a remarkable fact that the chromophore still exhibited efficient fluorescence in water, which is scarcely reported in previous literatures. Additionally, the chiral perturbation could also act on the involved excited state of the chromophore, making the emission of CPL possible.

3.4. CPL spectra of chiral alkyne architecture

The CPL (ΔI) and fluorescence spectra of chromophore in different solvents are compared (Fig. 5). It can be seen that the chromophore showed positive CPL signals. The sign of the CPL signal was the same to the sign observed in the CD spectra. This is the first example of CPL signals of chiral alkyne architecture. The CPL degrees of the chromophore were estimated by the luminescence dissymmetric factor (g_{lum}), which is defined as $g_{lum} = 2(I_L - I_R)/(I_L + I_R)$, where I_L and I_R are the intensities of left and right fluorescence emission [45]. The g_{lum} values for the chromophore in different solvents as a function of emission wavelength are displayed in Fig. 6. Interestingly, the dissymmetric factors of luminescence were comparable to those of absorption for the chromophore. This indicates there is no significant geometry change upon population of the excited state. This is further corroborated by the small Stokes shifts of the emission wavelengths. Compared to the reported CPL results of many chiral simple chromophores, helical nacre-like fibres [46] and CdS quantum dots prepared in a protein nanocage [47], our chiral alkyne architecture demonstrated similar g_{lum} values [2]. Though the g_{lum} values of chiral alkyne architecture are smaller than those of helically chiral 1,1′-bitriphenylenes ($\sim 10^{-2}$) [48], our results confirm that the constructed simple organic architecture is really able to produce the searched luminescent phenomenon in various solvents with different polarity, even in water. Additionally, the values of g_{abs} and g_{lum} for chiral alkyne architecture are also summarized in Table 1.

3.5. TP-CD of chiral alkyne architecture

Combined with increased penetrability of the near infrared excitation light and the confocal nature of TPA, TP-CD will be a useful tool for biomolecular identification [49]. Compared to one-photon excitation, two-photon excitation offers significant advantages for the biological fluorescence imaging and sensing which includes higher spatial resolution, less photobleaching and photodamage as well as deeper tissue penetration [50]. Considering that the alkyne link as π-bridge could result in efficient TPA and efficient chiroptical properties of our chromophore [51], so we also examined molecular TP-CD using theoretical calculations. The TP-CD spectrum of the chromophore is shown in Fig. 7. The first evident observation is that the chromophore indeed exhibits large TP-CD over most of the spectral range analyzed and the shape of the TP-CD spectrum resembles the linear absorption. Additionally, the TP-CD spectrum remains positive, which mimics the CD presented in Fig. 4.

4. Conclusions

In summary, we report the first example to achieve efficient CD and CPL in differently polar solvents from a water-soluble and violet-blue emissive organic chromophore. The design strategy is based on chiral perturbation in an achiral part, where the acting chromophore is alkyne architecture and the chirally perturbing moiety is proline. Although the reached g_{lum} values are in the typical range for simple organic molecules (typical $|g_{lum}| = 10^{-5}$–10^{-2}), this kind of water-soluble chiroptical molecule is still scarce but highly interesting family of the CPL organic molecules. Additionally, the chromophore exhibits large TP-CD in an wide spectral range from the theoretical calculations. This simple design opens up new perspectives for the future development of novel simple CPL organic dyes, as well as for the improvement of the CPL properties of the organic molecules spanning their use in photonic applications.

Acknowledgments

We thank the Natural Science Foundation of China (Grant nos. 11404219, 11404161, and 21402124), Natural Science Foundation of Guangdong Province (Grant no. 2014A030313552), Foundation for Distinguished Young Talents in Higher Education of Guangdong, China (FDYT, Grant no. 2014KQNCX127), Shenzhen Basic Research Project of Science and Technology under Grant (Nos. JCYJ20150324141711613) and the Key Laboratory of Optoelectronic Devices and Systems of Ministry of Education and Guangdong Province (GD201603).

Appendix A. Supplementary data

Supplementary data associated with this article can be found, in the online version, at https://doi.org/10.1016/j.synthmet.2017.10.008.

References

[1] J. Kumar, T. Nakashima, T. Kawai, Circularly polarized luminescence in chiral molecules and supramolecular assemblies, J. Phys. Chem. Lett. 6 (2015) 3445.
[2] E.M. Sanchez-Carnerero, A.R. Agarrabeitia, F. Moreno, B.L. Maroto, G. Muller, M.J. Ortiz, S. Moya, Circularly polarized luminescence from simple organic molecules, Chem. Eur. J. 21 (2015) 13488.
[3] G. Longhi, E. Castiglioni, J. Koshoubu, G. Mazzeo, S. Abbate, Circularly polarized luminescence: a review of experimental and theoretical aspects, Chirality 28 (2016) 696.
[4] H. Sato, T. Yajima, A. Yamagishi, Chiroptical studies on supramolecular chirality of molecular aggregates, Chirality 27 (2015) 659.
[5] S. Nishiyama, K. Urushibara, H. Masu, I. Azumaya, H. Kagechika, A. Tanatani, Conformational and chiral properties of cyclic-tri(N-methyl-meta-benzamide) bearing amidino groups, Chirality 27 (2015) 487.
[6] N. Nakayama, H. Goto, Theoretical electronic circular dichroism study of 1,3-Diene derivatives for the elucidation of ECD spectra of 1,3-Cyclohexadiene and its derivatives, Chirality 27 (2015) 476.
[7] T. Kinuta, K. Kamon, T. Harada, Y. Nakano, N. Tajima, T. Sato, M. Fujiki, R. Kuroda, Y. Matsubara, Y. Imai, Solid-state chiral supramolecular organic fluorophore having a π-conjugated phenylene ethynylene unit, Eur. J. Org. Chem. 2009 (2009) 5760.
[8] J. Jiménez, L. Cerdán, F. Moreno, B.L. Maroto, I. García-Moreno, J.L. Lunkley, G. Muller, S. de la Moya, Chiral organic dyes endowed with circularly polarized laser emission, J. Phys. Chem. C 121 (2017) 5287.
[9] Y. Sheng, J. Ma, S. Liu, Y. Wang, C. Zhu, Y. Cheng, Strong and reversible circularly polarized luminescence emission of a chiral 1, 8-Naphthalimide fluorophore induced by excimer emission and orderly aggregation, Chem. Eur. J. 22 (2016) 9519.
[10] F. Zinna, T. Bruhn, C.A. Guido, J. Ahrens, M. Bröring, L. Di Bari, G. Pescitelli, Circularly polarized luminescence from axially chiral BODIPY DYEmers: an experimental and computational study, Chem. Eur. J. 22 (2016) 16089.
[11] E.M. Sánchez-Carnerero, F. Moreno, B.L. Maroto, A.R. Agarrabeitia, M.J. Ortiz, B.G. Vo, G. Mullerand, S. Moya, Circularly polarized luminescence by visible-light absorption in a chiral O-BODIPY dye: unprecedented design of CPL organic molecules from achiral chromophores, J. Am. Chem. Soc. 136 (2014) 3346.
[12] S.-T. Wu, Z.-W. Cai, Q.-Y. Ye, C.-H. Weng, X.-H. Huang, X.-L. Hu, C.-C. Huang, N.-F. Zhuang, Enantioselective synthesis of a chiral coordination polymer with circularly polarized visible laser, Angew. Chem. Int. Ed. 53 (2014) 12860.
[13] T. Uchida, K. Nozaki, M. Iwamura, Chiral sensing of various amino acids using induced circularly polarized luminescence from Europium(III) complexes of phenanthroline dicarboxylic acid derivatives, Chem. Asian J. 11 (2016) 2415.
[14] F. Zinna, M. Pasini, F. Galeotti, C. Botta, L.D. Bari, U. Giovanella, Design of lanthanide-based OLEDs with remarkable circularly polarized electroluminescence, Adv. Funct. Mater. 27 (2014) 1603719.
[15] S. Feuillastre, M. Pauton, L. Gao, A. Desmarchelier, A.J. Riives, D. Prim, D. Tondelier, B. Geffroy, G. Muller, G. Clavierand, G. Pieters, Design and synthesis of new circularly polarized thermally activated delayed fluorescence emitters, J. Am. Chem. Soc. 138 (2016) 3990.
[16] Y. Wang, Y. Li, S. Liu, F. Li, C. Zhu, S. Li, Y. Cheng, Regulating circularly polarized luminescence signals of chiral binaphthyl-based conjugated polymers by tuning dihedral angles of binaphthyl moieties, Macromolecules 49 (2016) 5444.
[17] A.D. Merg, J.C. Boatz, A. Mandal, G. Zhao, S. Mokashi-Punekar, C. Liu, X. Wang, P. Zhang, P.C.A. van der Wel, N.L. Rosi, Peptide-directed assembly of single-helical gold nanoparticle superstructures exhibiting intense chiroptical activity, Am. Chem. Soc. 138 (2016) 13655.
[18] U. Tohgha, K.K. Deol, A.G. Porter, S.G. Bartko, J.K. Choi, B.M. Leonard, K. Varga, J. Kubelka, G. Muller, M. Balaz, Ligand induced circular dichroism and circularly polarized luminescence in CdSe quantum dots, ACS Nano 10 (2016) 8904.
[19] Y. Morisaki, M. Gon, T. Sasamori, N. Tokitohand, Y. Chujo, Planar chiral tetrasubstituted [2.2] paracyclophane: optical resolution and functionalization, J. Am.

Chem. Soc. 136 (2014) 3350.
[20] M. Gon, Y. Morisaki, R. Sawada, Y. Chujo, Synthesis of optically active X-shaped, conjugated compounds and dendrimers based on planar chiral [2.2]paracyclophane, leading to highly emissive circularly polarized luminescence, Chem. Eur. J. 22 (2016) 2291.
[21] J. Xiong, H. Feng, J. Sun, W. Xie, D. Yang, M. Liu, Y. Zheng, The fixed propeller-like conformation of tetraphenylethylene that reveals aggregation- induced emission effect chiral recognition, and enhanced chiroptical property, J. Am. Chem. Soc. 138 (2016) 11469.
[22] J. Yuasa, H. Ueno, T. Kawai, Sign reversal of a large circularly polarized luminescence signal by the twisting motion of a bidentate ligand, Chem. Eur. J. 20 (2014) 8621.
[23] Y. Sheng, D. Shen, W. Zhang, H. Zhang, C. Zhu, Y. Cheng, Reversal circularly polarized luminescence of AIE-Active chiral binaphthyl molecules from solution to aggregation, Chem. Eur. J. 21 (2015) 13196.
[24] J. Liu, H. Su, L. Meng, Y. Zhao, C. Deng, J.C.Y. Ng, P. Lu, M. Faisal, J.W.Y. Lam, X. Huang, H. Wu, K.S. Wong, B.Z. Tang, What makes efficient circularly polarised luminescence in the condensed phase: aggregation-induced circular dichroism and light emission, Chem. Sci. 3 (2012) 2737.
[25] T. He, S. Yao, J. Zhang, Y. Li, X. Li, J. Hu, R. Chen, X. Lin, Strong multiphoton absorption properties of one styrylpyridinium salt in a highly polar solvent, Opt. Express 24 (2016) 11091.
[26] T. He, Y. Wang, X. Tian, Y. Gao, X. Zhao, A.C. Grimsdale, X. Lin, H. Sun, An organic dye with very large stokes-shift and broad tunability of fluorescence: potential two-photon probe for bioimaging and ultra-sensitive solid-state gas sensor, Appl. Phys. Lett. 108 (2016) 011901.
[27] K. Hoffert, R.J. Durand, S. Gauthier, F. Robin-le Guen, S. Achelle, Synthesis and photophysical properties of a series of pyrazine-based push-pull chromophores, Eur. J. Org. Chem. 2017 (2017) 523.
[28] C. Huang, X. Peng, D. Yi, J. Qu, H. Niu, Dicyanostilbene-based two-photon thermosolvatochromic fluorescence probes with large two-photon absorption cross sections: detection of solvent polarities, viscosities, and temperature, Sens. Actuator B: Chem. 182 (2013) 521.
[29] C.L. Droumaguet, O. Mongin, M.H.V. Werts, M. Blanchard-Desce, Towards smart multiphoton fluorophores: strongly solvatochromic probes for two-photon sensing of micropolarity, Chem. Commun. 22 (2005) 2802.
[30] O.A. Kucherak, L. Richert, Y. Mély, A.S. Klymchenko, Dipolar 3-methoxychromones as bright and highly solvatochromic fluorescent dyes, Phys. Chem. Chem. Phys. 14 (2012) 2292.
[31] S. Sasaki, G.P.C. Drummen, G. Konishi, Recent advances in twisted intramolecular charge transfer (TICT) fluorescence and related phenomena in materials chemistry, J. Mater. Chem. C 4 (2016) 2731.
[32] T. He, Y. Gao, R. Chen, L. Ma, D. Rajwar, Y. Wang, A.C. Grimsdale, H. Sun, Multiphoton harvesting in an angular carbazole-containing Zn(II)-Coordinated random copolymer mediated by twisted intramolecular charge transfer state, Macromolecules 47 (2014) 1316.
[33] T. He, P.C. Too, R. Chen, S. Chiba, H. Sun, Concise synthesis and two-photon-excited deep-blue emission of 1, 8-diazapyrenes, Chem. Asian J. 7 (2095) (2012) 2090.
[34] T. He, Y. Gao, S. Sreejith, X. Tian, L. Liu, Y. Wang, H. Joshi, S.Z.F. Phua, S. Yao, X. Lin, Y. Zhao, A.C. Grimsdale, H. Sun, Biocompatible two-photon absorbing dipyridyldiketopyrrolopyrroles for metal-ion-mediated self-assembly modulation and fluorescence imaging, Adv. Opt. Mater. 4 (2016) 746.
[35] M. Shaikh, J. Mohanty, P.K. Singh, A.C. Bhasikuttan, R.N. Rajule, V.S. Satam, S.R. Bendre, V.R. Kanetkar, H. Pal, Contrasting solvent polarity effect on the photophysical properties of two newly synthesized aminostyryl dyes in the lower and in the higher solvent polarity regions, J. Phys. Chem. A 114 (2010) 4507.
[36] Y. Zhang, M. Jiang, G. Han, K. Zhao, B.Z. Tang, K.S. Wong, Solvent effect and two-photon optical properties of triphenylamine-based donor-acceptor fluorophores, J. Phys. Chem. C 119 (2015) 27630.
[37] J.A. Bautista, R.E. Connors, B.B. Raju, R.G. Hiller, F.P. Sharples, D. Gosztola, M.R. Wasielewski, H.A. Frank, Excited state properties of peridinin: observation of a solvent dependence of the lowest excited singlet state lifetime and spectral behavior unique among carotenoids, J. Phys. Chem. B 103 (1999) 8751.
[38] J.E. Field, G. Muller, J.P. Riehl, D. Venkataraman, Circularly polarized luminescence from bridged triarylamine helicenes, J. Am. Chem. Soc. 125 (2003) 11808.
[39] T. Nishikawa, N. Tajima, M. Kitamatsu, M. Fujiki, Y. Imai, Circularly polarised luminescence and circular dichroism of L- and D-oligopeptides with multiple pyrenes, Org. Biomol. Chem. 13 (2015) 11426.
[40] Y. Gobo, M. Yamamura, T. Nakamura, T. Nabeshima, Synthesis and chiroptical properties of a ring-fused BODIPY with a skewed chiral π skeleton, Org. Lett. 18 (2016) 2719.
[41] J. Kumar, T. Nakashima, H. Tsumatori, T. Kawai, Circularly polarized luminescence in chiral aggregates: dependence of morphology on luminescence dissymmetry, J. Phys. Chem. Lett. 5 (2014) 316.
[42] T. Ikeda, T. Masuda, T. Hirao, J. Yuasa, H. Tsumatori, T. Kawai, T. Haino, Circular dichroism and circularly polarized luminescence triggered by self-assembly of tris (phenylisoxazolyl)-benzenes possessing a perylenebisimide moiety, Chem. Commun. 48 (2012) 6025.
[43] S.V. Balasubramanian, J.L. Alderfer, R.M. Straubinger, Solvent- and concentration-dependent molecular interactions of taxol (Paclitaxel), J. Pharm. Sci. 83 (1994) 1470.
[44] H. Nakashima, M. Fujiki, J.R. Koe, M. Motonaga, Solvent and temperature effects on the chiral aggregation of poly(alkylarylsilane)s bearing remote chiral groups, J. Am. Chem. Soc. 123 (2001) 1963.
[45] A. Satrijo, S.C.J. Meskers, T.M. Swager, Probing a conjugated polymer's transfer of organization-dependent properties from solutions to films, J. Am. Chem. Soc. 128 (2006) 9030.
[46] J. Zhang, W. Feng, H. Zhang, Z. Wang, H.A. Calcaterra, B. Yeom, P.A. Hu, N.A. Kotov, Multiscale deformations lead to high toughness and circularly polarized emission in helical nacre-like fibres, Nat. Comm. 7 (2016) 10701.
[47] K. Iwahori, A. Miura, M. Yamane, I. Yamashita, M. Naito, Circularly polarized luminescent CdS quantum dots prepared in a protein nanocage, Angew. Chem. Int. Ed. 49 (2010) 7006.
[48] Y. Sawada, S. Furumi, A. Takai, M. Takeuchi, K. Noguchi, K. Tanaka, Rhodium-catalyzed enantioselective synthesis crystal structures, and photophysical properties of helically chiral 1,1′-bitriphenylenes, J. Am. Chem. Soc. 134 (2012) 4080.
[49] L.D. Boni, C. Toro, F.E. Hernández, Synchronized double L-scan technique for the simultaneous measurement of polarization dependent two-photon absorption in chiral molecules, Opt. Lett. 33 (2008) 2958.
[50] C. Ye, J. Zhang, X. Lin, T. Zhang, B. Wang, T. He, Multiphoton absorption of three chiral diketopyrrolopyrrole derivatives in near-infrared window I and II, Opt. Mater. Express 7 (2017) 3529.
[51] W. Hu, T. He, R. Jiang, J. Yin, L. Li, X. Lu, H. Zhao, L. Zhang, L. Huang, H. Sun, W. Huang, Q. Fan, Inner salt-shaped small molecular photosensitizer with extremely enhanced two-photon absorption for mitochondrial-targeted photodynamic therapy, Chem. Commun. 53 (2017) 1680.